

Study of Self-assembly for Mechanochemically-milled Saponite Nanoparticles

Kazuomi Numata, Kiminori Sato*, and Koichiro Fujimoto

Department of Environmental Sciences, Tokyo Gakugei University, 4-1-1 Koganei, Tokyo 184-8501, Japan

E-mail: sato-k@u-gakugei.ac.jp

(Received May 6, 2014)

The rheological mechanism of long-term self-assembly triggered by H₂O molecules was studied for unmilled and mechanochemically-milled saponite nanoparticles by means of thermogravimetry and differential thermal analysis (TG-DTA), dilatometry (DLT), and positronium (Ps) lifetime spectroscopy. For unmilled saponite, the adsorption of H₂O molecules due to hydration caused volume expansion arising from an increase in the basal spacing as well as weight gain with a time scale of ~10 h. Ps lifetime spectroscopy revealed two kinds of voids with sizes of ~0.3 nm and ~0.9 nm for unmilled saponite before hydration. The intensity of the larger void component in the annihilation spectra decreased from ~9 % to ~5 % with increasing time up to ~100 h and correspondingly the intensity of the smaller void component increased from ~5 % to ~9 % due to long-term rheological self-assembly. Both the weight gain and volume expansion were largely suppressed for milled saponite, indicating that the adsorption of H₂O molecules is reduced. Furthermore, the larger void disappeared and a single void component, corresponding to a void size slightly larger than the original smaller void, was formed for milled saponite. The intensity of this void, created as a result of destruction, decreased with increasing time up to ~100 h.

1. Introduction

Clay minerals are inorganic layered compounds consisting of two-dimensional (2D) nanosheets with angstrom-scale interlayer spaces. The 2D nanosheets are negatively charged due to the compositional and structural fluctuation. The negative layer charge is compensated by interlayer cations such as Na⁺ which attract to polarized H₂O molecules. Clay minerals can thus contain a large amount of H₂O molecule in the angstrom-scale interlayer spaces, which is characteristic for the swelling property [1]. It is known that 2D nanosheets spontaneously agglomerate with well-defined local structures through their mutual interactions with the aid of H₂O molecules. This agglomeration process toward structural densification, so-called self-assembly of 2D nanosheets, is increasingly of importance for dealing with global environmental issues [2–5]. For example, the local molecular structures appearing upon self-assembly have been found to play an important role in the Cs adsorption site [2, 3]. In a recent practical model of giant earthquake nucleation, the pore fluid of self-assembled geomaterials is associated with earthquake slip weakening in plate-boundary faults [4, 5].

Based on our recent findings using positronium (Ps) annihilation spectroscopy together with molecular dynamics (MD) simulation [6], the following rheological mechanism has been proposed for saponite clay minerals. Before self-assembly saponite clay minerals possess two kinds of local molecular structures, where one and two nanosheets are inserted into the interlayer spaces forming voids with sizes of ~0.3 nm and ~0.9 nm, respectively. H₂O molecules significantly trigger the self-assembly of saponite clay minerals. H₂O molecules adsorbed at the Na⁺ cations in the interlayer spaces act as a lubricant and are the driving force for the rheological motion of nanosheets parallel to the layer direction. One of the two nanosheets inserted into the interlayer spaces is thus released away. The local molecular structures with the larger voids are gradually altered to those with the smaller

voids which become dominant for self-assembled saponite clay minerals.

In the present study, self-assembly was studied for mechanochemically-milled saponite clay minerals by Ps lifetime spectroscopy coupled with thermogravimetry and differential thermal analysis (TG-DTA) and high-resolution dilatometry (DLT). We focus on the long-term self-assembly ranging from the onset of H₂O adsorption at the interlayer cations to far after complete hydration.

2. Experiments

Synthetic Na-type saponite samples with a particle size of approximately 45 nm in diameter (54.71 % SO₂, 5.02 % Al₂O₃, 0.03 % Fe₂O₃, 30.74 % MgO, 2.15 % Na₂O, 0.07 % CaO, 0.67 % SO₃, 6.64 % H₂O) produced by Kunimine Industries Co. Ltd., Japan were employed in this study. The as-received sample was mechanochemically milled with tungsten carbide balls for 9 h under dry atmosphere at ambient temperature. The particle size of the milled sample is expected to be smaller than that of the unmilled sample, although this could not be determined due to the particle agglomeration [7]. All the samples were dehydrated at 423 K for 12 h under a vacuum of $\sim 10^{-3}$ Pa, and after dehydration referred to as the starting sample. X-ray diffraction (XRD) pattern analysis confirmed the following structural features for the unmilled and milled saponite samples. The unmilled sample exhibits an XRD pattern typical of the 2 : 1 layered structure of saponite clay mineral, where the 2D nanosheets are periodically ordered. XRD peaks characteristic of the saponite layered structure were broadened for the milled sample, indicating that the 2D nanosheets are disordered due to fragmentation of the 2D nanosheets upon milling.

Adsorption of H₂O molecules was investigated with respect to the weight gain by means of TG-DTA (TG-DTA 2020SA, BRUKER AXS Co. Ltd.) at room temperature with α corundum (α Al₂O₃) as an internal standard. In parallel, length-change measurements were performed for uniaxially compacted samples with a high-precision differential-type dilatometer (TD5020SA, Bruker AXS) equipped with a closed-water-cycling system. The dilatometer system is fully cooled, keeping a constant temperature with high thermal stability and thus preventing temperature overshoot and runaway, which enables us to perform long-term measurements [8]. The starting samples were exposed to a humidity of ~ 35 % at a temperature of ~ 300 K, where the time-dependent data were obtained.

Ps lifetime spectroscopy was conducted to characterize the angstrom-scale open spaces. A fraction of energetic positrons injected into samples forms the positron-electron bound state, Ps. Singlet *para*-Ps (*p*-Ps) with the spins of the positron and electron antiparallel and triplet *ortho*-Ps (*o*-Ps) with parallel spins are formed at a ratio of 1 : 3. Hence, three possible positron states: *p*-Ps, *o*-Ps, and free positrons exist in the samples. The annihilation of *p*-Ps results in the emission of two γ -ray photons of energy 511 keV with a lifetime of ~ 125 ps. Free positrons are trapped by negatively charged parts, such as polar elements, and annihilate into two photons with a lifetime of ~ 450 ps. The positron in *o*-Ps undergoes two-photon annihilation with one of the electrons bound to surrounding molecules with a lifetime of a few ns after localization in angstrom-scale pores. The last process is known as *o*-Ps pick-off annihilation and provides information on the open space size R through its lifetime $\tau_{o\text{-Ps}}$ based on the Tao-Eldrup model [9, 10]:

$$\tau_{o\text{-Ps}} = 0.5 \left[1 - \frac{R}{R_0} + \frac{1}{2\pi} \sin \left(\frac{2\pi R}{R_0} \right) \right]^{-1} \quad (1)$$

where $R_0 = R + \Delta R$, and $\Delta R = 0.166$ nm is the thickness of homogeneous electron layer in which the positron in *o*-Ps annihilates.

The positron source (²²Na), sealed in a thin foil of Kapton, was mounted in a sample-source-sample sandwich. The starting samples were exposed to a relative humidity of ~ 35 % at ambient temperature, and Ps lifetime measurements were performed every 45 min during hydration. The validity of our lifetime measurements and data analysis was confirmed with certified reference materials (NMIJ CRM 5601-a and 5602-a) provided by the National Metrology Institute of Japan, National In-

stitute of Advanced Industrial Science and Technology (AIST) [11, 12]. Positron lifetime spectra were numerically analyzed using the POSITRONFIT code [13]. The relative intensity of the *o*-Ps pick-off annihilation component, evaluated from an analysis of the positron lifetime spectrum was regarded as the fraction of open space.

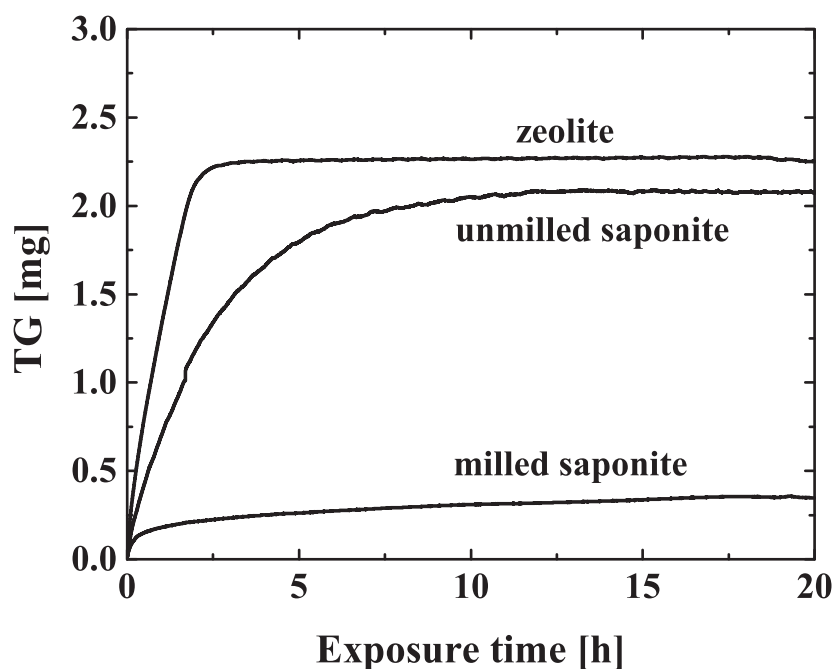


Fig. 1. Thermogravimetry (TG) data of unmilled and milled saponite samples as a function of exposure time. The data for zeolite sample is added for comparison.

3. Results and discussions

Figure 1 shows time-dependent thermogravimetry (TG) for unmilled and milled saponite samples. The data for zeolite is added as well for comparison. The TG data for unmilled saponite gradually increases with increasing exposure time up to ~ 8 h owing to hydration in the interlayer spaces and is saturated thereafter. The TG data for zeolite increase more rapidly with exposure time up to ~ 2 h and stays constant thereafter. This demonstrates that adsorption of H_2O molecules is greater in zeolite than in saponite. A similar time variation of TG is obtained for milled saponite, but the saturated TG value is much lower than that of unmilled saponite, demonstrating that adsorption of H_2O molecules is reduced for milled saponite.

Figure 2 shows length changes as a function of exposure time obtained for the unmilled and milled saponite samples. For the unmilled saponite sample, the macroscopic length change due to volume expansion exhibits a time scale similar to that of the TG-DTA data microscopically occurring at interlayer spaces (see Fig. 1). As mentioned in the experimental section, the present saponite samples are uniaxially compacted for the length-change measurements with DLT. It is thus expected that the 2D nanosheets are well ordered as illustrated in the inset of Fig. 2. H_2O adsorption in the interlayer spaces locally expands basal spacing as has been assessed by XRD under controlled relative humidity conditions [14]. It is therefore reasonable that the data for time-dependent length change is consistent with that of TG-DTA. It is noted that volume expansion is largely suppressed for milled saponite. Expansion of basal spacing with the fragmented 2D nanosheets could contribute less to the

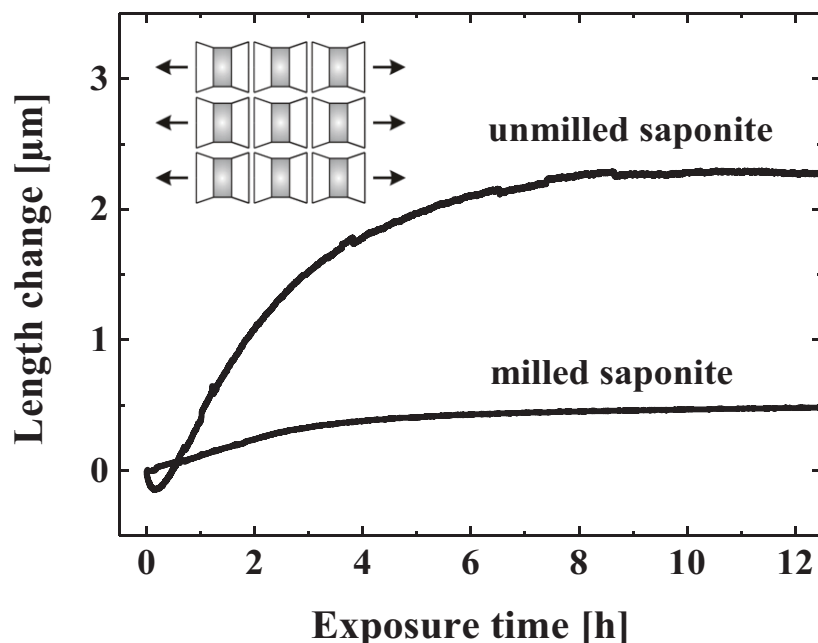


Fig. 2. Length changes as a function of exposure time obtained for the unmilled and milled saponite samples.

macroscopic volume change.

Ps lifetime spectroscopy for both unmilled saponite and zeolite revealed two kinds of voids, a smaller void labeled A and a larger void labeled B, whereas only a small void was observed for milled saponite. For unmilled saponite, the smaller void A had a radius of ~ 0.3 nm which was unchanged with exposure time. For milled saponite, the smaller void A had a radius slightly larger than ~ 0.3 nm prior to self-assembly and the radius decreases down to ~ 0.3 nm, similar to that of unmilled saponite, with increasing exposure time. The radius of the larger void B for unmilled saponite decreased significantly from ~ 0.9 nm to ~ 0.6 nm with increasing exposure time, whereas the void size of B for milled saponite (~ 0.6 nm) was unchanged with exposure time. The radius of the smaller void for zeolite was ~ 0.3 nm, corresponding to a β cage. The radius of the larger void for zeolite was ~ 0.5 nm, corresponding to an α cage.

Figure 3 shows the measured fractional intensity of each void obtained for both the unmilled and milled saponite samples as a function of exposure time. The data for zeolite is also added for comparison. The fraction of the smaller void for zeolite quickly increases from ~ 7 % to ~ 13 % with increasing exposure time along with a decrease of the larger void from ~ 12 % to ~ 0 . The larger void was not observed after an exposure time of 2.5 h, which is consistent with the TG data (see Fig. 1). This behaviour is typical of Ps annihilation occurring in water, which fills the α and β cages [15]. The present Ps lifetime spectroscopy results, together with the TG-DTA data, clearly capture the picture that the weight increase due to hydration observed for zeolite solely arises from the occupation of α and β cages by H_2O molecules.

In contrast to zeolite, the fraction of the smaller void A for unmilled saponite slowly increases from ~ 5 % to ~ 9 % with increasing exposure time together with a decrease of the larger void from ~ 9 % to ~ 5 %. The change takes place on a time scale of ~ 100 h, much longer than that of TG-DTA with a time scale of ~ 8 h. It is thus concluded that the long-term molecular dynamics probed by Ps lifetime spectroscopy originates from the self-assembly of 2D nanosheets rheologically caused by H_2O molecules. Milled saponite indicates a completely different time variation for the fractions of

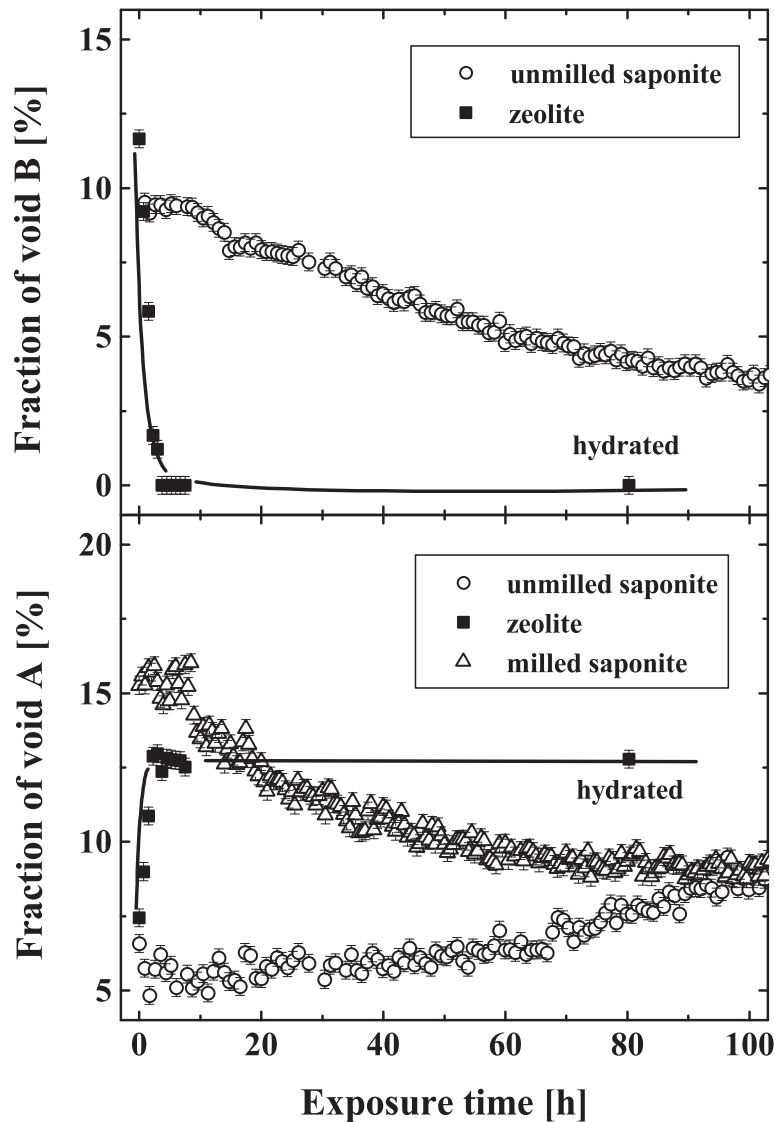


Fig. 3. Fractions of small and large voids obtained for the unground and milled saponite samples (open symbols) as a function of exposure time. The data for zeolite (solid symbols) is also added for comparison.

the smaller and larger voids A and B. The fraction of the smaller void A is $\sim 16\%$ before hydration, which is significantly higher than for unground saponite. It decreases from $\sim 16\%$ to $\sim 9\%$ with a time scale of ~ 100 h.

Previously, we conducted molecular dynamics (MD) calculations to figure out the location of the two kinds of voids for unground saponite [6]. One of the molecular structures is called type A, in which one 2D nanosheet is inserted into the interlayer spaces forming a void with a size of ~ 0.3 nm, as illustrated on the left hand side of Fig. 4. Another is type B, in which two 2D nanosheets are inserted into the interlayer spaces forming a large void with a size of ~ 0.9 nm (see the right hand side of Fig. 4). Note that the sizes of voids simulated by MD calculations are in agreement with those observed by Ps annihilation spectroscopy. The results of Ps lifetime spectroscopy thus demonstrate that the local molecular structure denoted as type A with the smaller void increases maintaining its size along with self-assembly. On the other hand, the local structure of type B disappears with

self-assembly shrinking this larger void. Type A could be an intrinsic local molecular structure of unmilled saponite, whereas the type B could be a metastable structure present dominantly prior to self-assembly. It is reasonably inferred for unmilled saponite that the metastable structure of type B is gradually altered to the intrinsic structure of type A together with self-assembly.

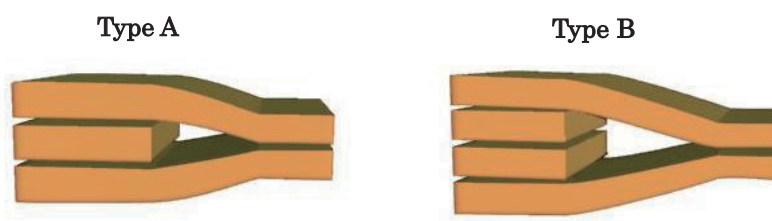


Fig. 4. Schematic illustrations of two kinds of local molecular structures, types A and B.

The larger void B disappeared for milled saponite. In addition, a void is introduced as a result of destruction by milling, as deduced from the increase of the fraction of the smaller void A (see Fig. 3). As mentioned above, the positron lifetime corresponding to the void A is slightly longer for milled saponite prior to self-assembly. It is thus expected that the size of the void introduced by milling is slightly larger than that of the smaller void A. The small void introduced by milling decreases down to that of unmilled saponite with increasing time, being a metastable state. For milled saponite, self-assembly altering the local molecular structures from type B to type A proceeds together with the disappearance of metastable voids. After the disappearance of metastable voids, self-assembly exclusively governs the structural modification. The fraction of void A for milled saponite could thus go back to that of unmilled saponite after long-term self-assembly.

Based on the present findings of Ps annihilation spectroscopy together with TG-DTA and DLT, the following rheological mechanism of self-assembly induced by H₂O molecules can be drawn for the unmilled and milled saponite samples. Prior to self-assembly saponite nanoparticles possess two kinds of local molecular structures, types A and B, where one and two nanosheets are inserted into the interlayer spaces forming voids with radii of ~0.3 nm and ~0.9 nm, respectively. Types A and B correspond to the intrinsic and metastable local molecular structures, respectively. H₂O molecules trigger off the self-assembly of saponite nanoparticles. H₂O molecules adsorbed at the Na⁺ cations in the interlayer spaces act as a lubricant, and are the driving force for the rheological motion of the nanosheets in parallel to the layer direction. One of the two nanosheets inserted into the interlayer spaces is thus released away. The local molecular structures with larger voids are gradually altered to those with smaller voids that finally become dominant for the self-assembled saponite nanoparticles. For milled saponite, the 2D nanosheets are highly disordered owing to fragmentation. The local molecular structure of type B cannot be maintained with the finely disordered 2D nanosheets. Furthermore, voids with a size slightly larger than that of type A with 0.3 nm are formed as a result of destruction by milling. This void is metastable and gradually disappears.

4. Conclusion

The rheological mechanism of long-term self-assembly induced by H₂O molecules was investigated for unmilled and mechanochemically-milled saponite. The unmilled saponite possesses two kinds of local molecular structures, where one and two nanosheets are inserted into interlayer spaces forming voids with sizes of ~0.3 nm and ~0.9 nm, respectively. During hydration, the fractional intensity of each type of void for the unmilled saponite varies with a time scale of ~100 h, which is much longer than the change in TG-DTA, which has a time scale of ~8 h. This long-term molecular dy-

namics probed by Ps annihilation spectroscopy thus originates from the self-assembly of saponite nanoparticles. In the process of self-assembly, H₂O molecules adsorbed at Na⁺ cations in the interlayer spaces cause the rheological motion of 2D nanosheets in parallel to the layer direction. One of two nanosheets inserted into the interlayer spaces is gradually released away, and the local molecular structure with smaller voids becomes dominant for the self-assembled saponite. The 2D nanosheets for milled saponite are highly disordered due to fragmentation. The local molecular structure with larger voids cannot be thus maintained. Furthermore, voids with a size slightly larger than 0.3 nm are introduced as a result of destruction by milling. This void is metastable and its fractional intensity gradually decreases with increasing exposure time.

Acknowledgment

The authors are indebted to K. Kawamura (Okayama University) for fruitful discussion. This work was partially supported by a Grant-in-Aid of the Japanese Ministry of Education, Science, Sports and Culture (Grant Nos. 25400318 and 25400319).

References

- [1] P. Porion, L. J. Michot, A. M. Faugère, and A. Delville: *J. Phys. Chem. C* **111** (2007) 5441.
- [2] K. Numata, K. Sato, and K. Fujimoto: *Int. J. Nanosci.* **11** (2012) 1240034.
- [3] K. Sato, K. Fujimoto, W. Dai, and M. Hunger: *J. Phys. Chem. C* **117** (2013) 14075.
- [4] C. A. J. Wibberley and T. Shimamoto: *Nature* **436** (2005) 689.
- [5] K. Sato, K. Numata, and K. Fujimoto: *Int. J. Nanosci.* **11** (2012) 1240033.
- [6] K. Sato, K. Fujimoto, K. Kawamura, W. Dai, and M. Hunger: *J. Phys. Chem. C* **116** (2012) 22954.
- [7] K. Sato, K. Numata, W. Dai, and M. Hunger: *Phys. Chem. Chem. Phys.* **16** (2014) 10959.
- [8] K. Sato and W. Sprengel: *J. Chem. Phys.* **137** (2012) 104906.
- [9] S. J. Tao: *J. Chem. Phys.* **56** (1972) 5499.
- [10] M. Eldrup, D. Lightbody, and J. N. Sherwood: *Chem. Phys.* **63** (1981) 51.
- [11] K. Ito, T. Oka, Y. Kobayashi, Y. Shirai, K. Wada, M. Matsumoto, M. Fujinami, T. Hirade, Y. Honda, H. Hosomi, Y. Nagai, K. Inoue, H. Saito, K. Sakaki, K. Sato, A. Shimazu, and A. Uedono: *Mater. Sci. Forum* **607** (2009) 248.
- [12] K. Ito, T. Oka, Y. Kobayashi, Y. Shirai, K. Wada, M. Matsumoto, M. Fujinami, T. Hirade, Y. Honda, H. Hosomi, Y. Nagai, K. Inoue, H. Saito, K. Sakaki, K. Sato, A. Shimazu, and A. Uedono: *J. Appl. Phys.* **104** (2008) 026102.
- [13] P. Kirkegaard and M. Eldrup: *Computer Phys. Commun.* **7** (1974) 401.
- [14] S. Morodome and K. Kawamura: *Clays Clay Miner.* **57** (2009) 150.
- [15] A. M. Habrowska and E. S. Popiel: *J. Appl. Phys.* **62** (1987) 2419.